

X-ray Emission from GPS and CSS Sources

Aneta Siemiginowska^{1,*}

Harvard-Smithsonian Center for Astrophysics, 60 Garden St., Cambridge, MA 02138, USA

The dates of receipt and acceptance should be inserted later

Key words X-rays: galaxies - active, jets - radio

Many X-ray observations of GigaHertz Peaked Spectrum and Compact Steep Spectrum sources have been made with Chandra X-ray Observatory and XMM-Newton Observatory over the last few years. The X-ray spectra contribute the important information to the total energy distribution of the compact radio sources. In addition the spatial resolution of Chandra allows for studies of the X-ray morphology of these sources on arcsec scales and provide a direct view of their environments. This paper gives a review of the current status of the X-ray observations and their contribution to our understanding of the nature of these compact radio sources. It also describes primary physical processes that lead to the observed X-ray emission and summarize X-ray emission properties expected from interactions between an expanding radio source and the intergalactic environment.

© 2006 WILEY-VCH Verlag GmbH & Co. KGaA, Weinheim

1 Introduction

A standard picture of a radio source shows a large scale emission in forms of lobes and hot spots that are often connected to the radio core by narrow jets. Such emission spans hundreds of kiloparsecs and can be studied in details in nearby sources, for example in the closest powerful FR II radio source Cygnus A (FR II, $z = 0.056$). However, the morphology of the X-ray emission is very different. The *Chandra* X-ray Observatory image of Cygnus A (Wilson, Young & Shopbell 2000, Smith et al. 2002) shows a more circular diffuse X-ray emission surrounding the radio source with two prominent hot spots and a filamentary structure. A primary source of this X-ray emission is a hot (a few keV) thermal cluster gas, while the radio emission is mainly due to non-thermal particles accelerated in the jet, lobes and hot spots.

The nearby (3.7 Mpc) radio source Centaurus A is much smaller than Cygnus A. It has a double lobe radio structure only slightly larger than its host galaxy. The source morphology is very rich, showing an absorbed core, dust lanes, jet, counter-jet, radio lobes and shocks in multi-wavelength observations. X-ray emitting components can be resolved in X-rays because of the source proximity. They provide critical information about the physics and processes that are happening in this source (e.g. Kraft et al. 2007). GPS radio sources are embedded within the host galaxy and their multi-wavelength morphology might be similar to Cen A. However, if they are more distant their X-ray components may not be resolved.

What type of processes can generate an X-ray emission? Thermal emission is associated with a hot plasma with temperatures of a few keV and is observed in clusters of galax-

ies or halos of some active galaxies. There have been some failed attempts to detect such emission surrounding GPS sources in the past searches for a “confinement medium” of the radio source (Antonelli & Fiore 1997, O’Dea et al. 2000, Siemiginowska et al. 2003) in the past. Non-thermal emission associated with relativistic particles requires acceleration processes and is observed in jets, or shock regions resulting from interactions between the radio source and the ISM. Relativistic particles emit radio synchrotron photons and radio observations can give information about the distribution of particles. X-ray synchrotron emission requires very high energy electrons ($\gamma \sim 10^7 - 10^8$) that have short (~ 10 years) synchrotron life times. Therefore any X-ray synchrotron emission requires an on-going re-acceleration process.

Studies of interactions between the radio source and the interstellar and intergalactic medium can provide information about the energy that is deposited into the IGM by the expanding radio source. This is important to our understanding of the feedback process. GPS/CSS sources are observed at the early stage of their growth, where such interactions are strong. In addition theoretical models predict that a relatively strong X-ray emission should be associated with GPS and CSS sources.

2 X-ray Emission of Radio Sources: Models

There are several theoretical predictions of the X-ray emission from evolving radio sources. Begelman & Cioffi (1989) following Scheuer (1974), draw a general picture of an evolving radio source where the shocked IGM creates an overpressured cocoon surrounding a double radio structure with lobes, jets and a bow shock bounding the cocoon. The shock heated material emits X-rays. Reynolds, Heinz & Begelman (2001) present numerical simulations of a radio

* Corresponding author: e-mail: asiemiginowska@cfa.harvard.edu

source expansion within a uniform medium with three phases of the evolution: a supersonic cocoon, subsonic sideways expansion with a weak shock and supersonic jet, and a final sonic boom phase. Each phase is characterized by a different morphology of the X-ray emitting gas that is being heated by the expanding source. Sutherland & Bicknell (2007a, 2007b) shows a similar view of the radio source evolution within a clumpy medium (see also Bicknell & Sutherland 2006). Also in this simulations the X-ray emission is the result of interactions and the X-ray luminosity depends on the density and clumpiness of the medium. They discuss the time dependent (0.1-10 keV) X-ray emissivity with the maximum of the X-ray luminosity reached within the first few $\sim 10^4$ years.

Heinz, Reynolds & Begelman (1998) consider an evolution of GPS sources within the uniform environment of the host galaxy. The simulated X-ray surface brightness shows the shock discontinuity moving outwards with time. X-ray detections of such discontinuity require high spatial resolution and dynamic range observations in nearby sources. The shock of Cen A is seen as a factor of ~ 10 jump at ~ 7 kpc away from the nucleus and it is ~ 600 pc wide (Kraft et al. 2007). It has not been detected in any observations of GPS sources so far, possibly due to the requirement of high signal-to-noise data and spatial resolution that have not been obtained in the existing observations.

Recently Stawarz et al. (2008) presented a spectral emission model for GPS sources (see also Ostorero et al. in this Proceedings). The main contribution to the spectral energy distribution comes from the radio lobes and hot spots of the < 1 kpc size radio source embedded in the radiation field of the host galaxy. The X-ray emission is due to Inverse Compton scattering off the relativistic electrons within the radio source. The UV-disk photons and IR-dust photons provide the external radiation field to the hot spots, lobes and jet. This field dominates in smaller sources, while the synchrotron photon field intrinsic to the lobes dominates in larger sources, and GPS/CSS sources exceeding 1 kpc in size will be dominated by the synchrotron self-Compton emission process in the X-ray band. The predicted X-ray luminosity depends on a few model parameters such as a jet power, photon fields and the density of the ISM. Note that this model relates the X-ray emission to the radio source components while the simulations described above consider the emission from the hot gas heated by the radio source.

Both type of the X-ray emission, thermal and non-thermal, will be present in GPS sources. Hot thermal gas will produce an X-ray spectrum with emission lines, while the non-thermal continuum does not have any spectral features. High resolution X-ray spectra are needed in order to disentangle these two emission components.

3 X-ray Observations of GPS/CSS Sources

Before *Chandra* and *XMM-Newton* there was only one GPS galaxy detected in X-rays by ASCA (O'Dea et al. 2000) and

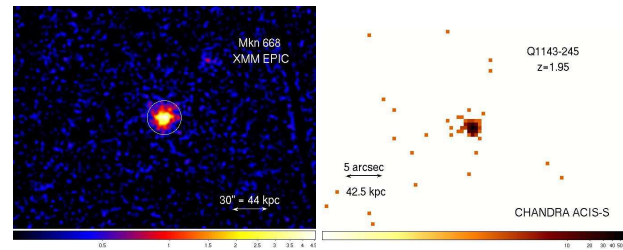


Fig. 1 **Left:** *XMM-Newton* EPIC X-ray image of Mkn668 ($z=0.076$). A $30''$ radius circle is marked around the source. The source is unresolved on this scale. A $30''$ scale bar equivalent to 44 kpc is shown in the right corner. **Right:** *Chandra* ACIS-S image of Q1143-245 at $z=1.95$. $5''$ scale corresponding to 42.6 kpc at the source redshift is marked in the left corner. Note that the radio source size is much smaller than the resolution of these two instruments.

several GPS quasars detected with HEAO-1 and ROSAT (see O'Dea 1998 for a summary). During the last decade there have been several efforts to increase the number of X-ray detections. Guainazzi et al. (2004, 2006) and Vink et al. (2006) present X-ray samples of GPS galaxies, Siemiginowska et al. (2003, 2005, 2008) discuss X-ray emission in GPS/CSS quasars. Worrall et al. (2004) and O'Dea et al. (2006) study details of the X-ray emission in a single GPS source.

Chandra and *XMM-Newton* observational capabilities are complementary. *Chandra* exceptional point spread function (PSF) allows for studies of X-ray morphology with ~ 1 arcsec resolution and the highest dynamic range available in the X-ray band today (Van Speybroeck et al. 1997, Weiskopf et al. 2000). Because of its low background it gives efficient detections of very faint sources and relatively good quality spectra within 0.5-7 keV. The PSF of the *XMM-Newton* is too large for studies of the X-ray morphology of GPS sources (Kirsch et al. 2004), but a very high effective area of the telescope gives high quality spectra within 0.5-10 keV energy range.

The spatial resolution of modern X-ray telescopes is still much worse than the resolution obtained by radio observations. Figure 1 shows the X-ray image of a nearby GPS source Mkn 668 at $z=0.076$ ($1 \text{ arcsec} = 1.46 \text{ kpc}$). A double radio structure ($< 10 \text{ pc}$) is fully enclosed within the X-ray point source observed with *XMM-Newton* EPIC camera. The highest redshift GPS source in the X-ray sample is plotted in Figure 2. Q1143-245 ($z=1.95$) is an unresolved X-ray point source in the *Chandra* ACIS-S observation and $1.5''$ corresponds to $\sim 12 \text{ kpc}$ at the quasar distance.

Table 1 lists the physical size in kpc for a source located at different redshifts. 1 arcsec corresponds to a physical size of 179 parsec in Cen A, while it corresponds to 8 kpc for a source at redshift 1. The redshift distribution for a sample of sources observed so far in X-rays is plotted in Figure 2. The peak distribution of the GPS galaxies is at $z \sim 0.3 - 0.4$ and for a radio source smaller than $< 10 \text{ kpc}$ cannot be resolved with the current X-ray telescopes. For the GPS quasars the

Table 1 Physical Size vs. Redshift

Redshift	1'' kpc	5'' kpc	Example GPS Source
0.00087	0.0179	0.0895	Cen A
0.01	0.202	1	
0.076	1.46	7.3	Mkn 668
0.1	1.8	9	
0.668	7	35	0108+338
1	8	40.7	

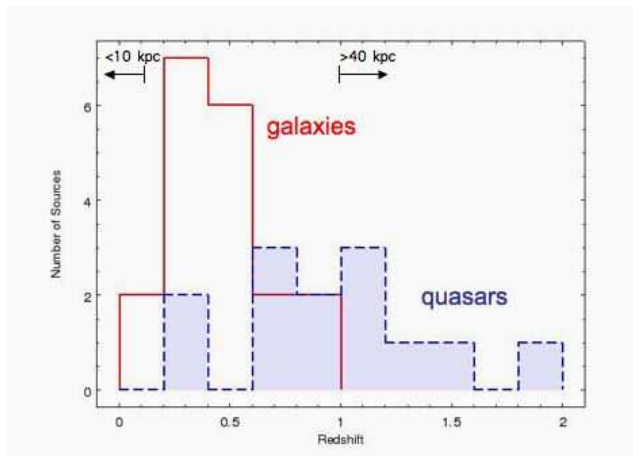


Fig. 2 Redshift distribution of GPS and CSS sources observed in X-rays. The histogram includes both *Chandra* and *XMM-Newton* observations and consists of 19 galaxies and 13 quasars. The galaxies are marked by a solid red line and quasars by a dashed blue line and a shaded region. 5'' scale corresponding to size < 10 kpc and > 40 kpc is marked by arrows. The data points are from Guainazzi et al. (2004, 2006), Vink et al. (2006) and Siemiginowska et al. (2008).

distribution spans evenly the redshift between 0.4 – 2. At redshift $z > 1$ the 5 arcsec size of a point source contains a source exceeding > 40 kpc in size. GPS radio structure is smaller than < 1 kpc, CSS < 10 kpc, so any associated X-ray emission (as in Stawarz et al. 2008 model) would not be resolved.

An unresolved X-ray point source will contain a source smaller than $< 3''$ in *Chandra* and $< 15''$ in *XMM-Newton* observations. There, in most GPS/CSS we can only study X-ray spectral properties and may be able to disentangle different emission components, evaluate absorption properties and intrinsic source luminosity. However, an X-ray emission on scales larger than the PSF size can be studied with *Chandra* in nearby sources (see Fig. 2), e.g. a diffuse emission associated with cocoon, Narrow Emission Line regions, super winds, X-ray cluster or relic emission. In addition larger scale jets associated with the radio source could be detected if their length exceeds $> 3''$.

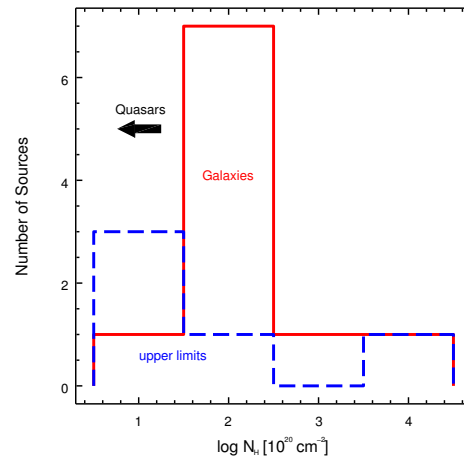


Fig. 3 Distribution of the intrinsic absorption column in GPS galaxies. The histogram includes both *Chandra* and *XMM-Newton* observations from Guainazzi et al. (2004, 2006), Vink et al. (2006), Siemiginowska et al. 2008, Tengstrand et al. (2008). Detections are plotted with the solid red curve and upper limits with the dashed blue curve. The observed columns in GPS quasars reported by Siemiginowska et al. (2008) are marked by a big arrow and all are below $N_H < 10^{21}$ atoms cm^{-2} .

3.1 Compact Source: X-ray Spectra

GPS sources are faint in X-rays and have varying quality of the X-ray spectrum, from a detection of a source with just a few counts in a short ~ 5 ksec *Chandra* exposure to a relatively good spectra with > 1000 counts in a longer 20-30 ksec *XMM-Newton* observations. Most spectra do not show any strong emission lines, except for Mkn 668 (Guainazzi et al. 2004), and can be characterized by an absorbed power law model. Such a model provides an estimate of an X-ray flux and probes the X-ray absorption properties.

Figure 3 shows a distribution of the intrinsic absorption column in GPS galaxies observed so far in X-rays. There is a peak at $\sim 10^{22}$ atoms cm^{-2} in the distribution and most of the galaxies are absorbed in X-rays. On the other hand the quasars show no intrinsic absorption with detection limits below $< 10^{21}$ atoms cm^{-2} (Siemiginowska et al. 2008). The GPS galaxies show an anticorrelation between the X-ray absorption column and the radio source size (Guainazzi et al. 2006, Vink et al. 2006) similar to the one noticed in the observations of HI 21 cm absorption by Pihlström, Conway & Vermeulen (2003). This may indicate an evolutionary phase in radio source growth in which the initially enshrouded nucleus is being “clear out” by an expanding radio source.

Given the X-ray spectra and the observed absorbing column one can determine the source intrinsic X-ray luminosity. The new observations indicate that the GPS galaxies are not X-ray quiet. Their X-ray luminosity corrected for

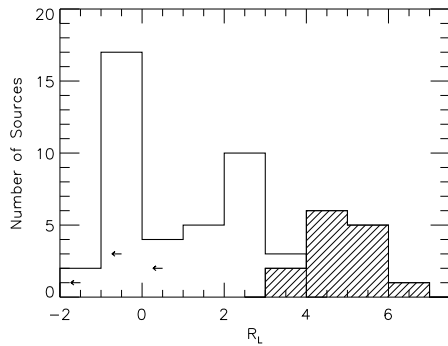


Fig. 4 Radio loudness of the GPS quasars from Siemiginowska et al.(2008) compared to the other radio-loud quasars from Elvis et al.(1994). GPS/CSS quasars are marked by shaded histogram and they are more radio loud.

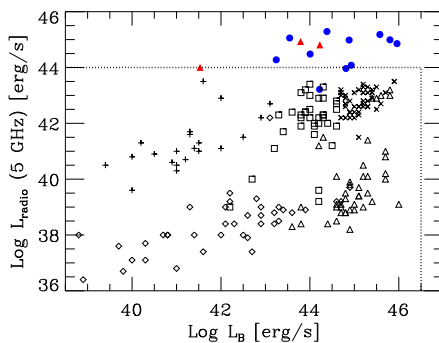


Fig. 5 Radio loudness in comparison to the B-band luminosity for a different classes of sources in Sikora et al. (2007). The location of the GPS quasars (circle) and galaxies (triangle) is marked on the original diagram of Sikora et al. Most GPS sources are more radio loud, optically brighter and located outside a range (marked by a dashed line) observed in the other sources. Note B-luminosity for GPS galaxies is typically undetermined, because of the intrinsic absorption of the nucleus.

absorption exceeds 10^{42} ergs s^{-1} and matches the X-ray luminosities of GPS quasars and FR II type radio galaxies (Guainazzi et al.2006, Tengstrand et al. 2008).

With the new observations we can also study the spectral energy distribution of the GPS sources from radio to X-rays. Such analysis indicate that the GPS/CSS quasars are more radio loud than the other radio loud quasars (see Fig. 4), where the radio loudness is defined as a ratio between the radio and optical (B band) luminosity. A comparison with a larger sample of variety of radio loud objects in Sikora, Stawarz & Lasota (2007) shows that the GPS quasars and galaxies are most radio luminous for a given optical luminosity (see Fig. 5). This may suggest a higher radiative efficiency in a younger (smaller) GPS source as postulated by the theory (see Begelman, 1997).

We can summarize the main observational results based on the X-ray spectra:

- Absorption: (1) high ($> 10^{22}$ cm $^{-2}$) column densities are common in galaxies; (2) there is a tentative dependence of the column density on the distance between the hot spots/lobes X-ray; (3) X-ray column density is always larger than the HI column observed in radio.
- Intrinsic X-ray Luminosity: (1) GPS galaxies are not X-ray quiet; (2) GPS/CSS quasars show an indication that they are X-ray weak.
- X-ray loudness: (1) X-ray to radio luminosity ratios are similar to the ratios observed in FRI galaxies; (2) GPS/CSS quasars are the most radio loud objects.

3.2 X-ray Morphology (on kpc scales)

GPS radio structure is much smaller than the spatial resolution capabilities of the current X-ray instruments, so the GPS source remains unresolved (even in the lowest redshift sources) in all X-ray observations to date. X-ray morphology on scales exceeding the GPS source size can be studied with *Chandra*. Several types of X-ray morphology have been detected in the GPS and CSS sources:

- X-ray jets were detected on large scales up to hundreds kpc away from the GPS source: PKS1127-145 (Siemiginowska et al. 2002, 2007), B2 0738+393 (Fig.6, Siemiginowska et al. 2003).
- an irregularly shaped diffuse X-ray emission: PKS B1345+125 (Siemiginowska et al. 2008, Guainazzi et al. in preparation)
- a secondary X-ray emission associated with a radio source located $20''$ to the west of a double nucleus GPS galaxy PKS 0941-080 (Siemiginowska et al. 2008)
- an X-ray emission associated with a cluster of galaxies at the GPS source redshift: CSS quasar 3C186 is in the center of an X-ray cluster (Siemiginowska et al. 2005)

A large scale X-ray emission associated with the GPS source may also indicate intermittency of a central AGN. Baum et al. (1990) postulated that an extended radio emission detected $\sim 20''$ away from the GPS galaxy 0108+388 is a relic of an earlier active phase of the source. Reynolds & Begelman (1997) argued that intermittent activity can explain the observed statistics of GPS sources. Intermittency or “modulated jet activity” has been considered as a mechanism shaping the morphology of large scale jets (for details see Stawarz et al. 2004 and examples: 3C273 by Stawarz 2004, and Jester et al. 2006; PKS1127-145 Siemiginowska et al. 2007). The newborn portion of the jet resembles the GPS source, but at later time it will be observed as a knot in the extended jet.

A large scale emission allows also for studies of interactions between the radio source and the environment. A detection of an X-ray cluster in the *Chandra* observation of 3C186 (Fig.7) provided a way to study the surroundings of the radio source. The measured temperature and density

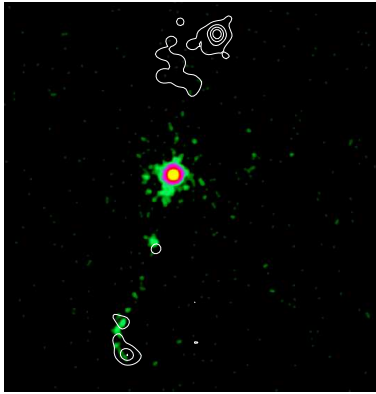


Fig. 6 A smoothed *Chandra* ACIS-S (0.3-7 keV) image of B2 0738+393 overlaid with the radio contours (VLA-1.4 GHz). The X-ray jet is narrow, curves and follows the radio structure to the south. The jet ends with a hot spot at the southernmost part of the radio lobe. A knot at ~ 13 arcsec away from the core and its emission is consistent with the X-rays being created by the inverse Compton scattering of the cosmic microwave background (CMB) photons and requires jet bulk Lorentz factors of a few ($\Gamma_{bulk} \sim 5 - 7$) (see Siemiginowska et al. (2003) for details).

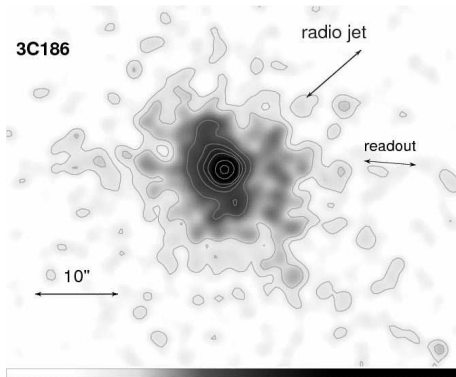


Fig. 7 Smoothed *Chandra* ACIS-S (0.3-7 keV) image of 3C 186. The diffuse cluster emission extends to ~ 120 kpc from the central quasar. The 10 arcsec (82 kpc) size is marked. The direction of an unresolved 2 arcsec radio jet is also marked.

of the X-ray emitting hot cluster gas allow for an estimate of the gas pressure. This in turn could be compared to the pressure measured in the radio lobes. In 3C186 the pressure in the radio lobes exceeded the thermal gas pressure by 2 orders of magnitude (Siemiginowska et al. 2005). This observation therefore allowed to conclude that the jet is not frustrated and the radio source expands with no disruptions.

Fig. 8 shows smoothed *Chandra* ACIS-S images of PKS B1345+125 in the soft (0.5-2 keV) and hard (2-10 keV) bands. The diffuse X-ray emission seen in the soft band may originate as a thermal emission associated with the galaxy halo. Its size agrees with the size of the extended optical line region studied kinematically in the optical and described by

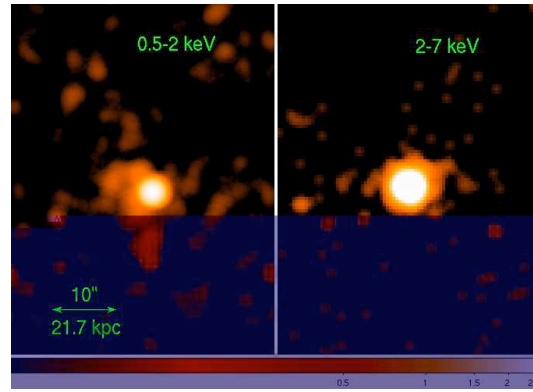


Fig. 8 Smoothed *Chandra* ACIS-S images of PKS 1345+125. **Left:** The soft (0.5-2 keV) band showing the extended emission surrounding the core. The $10''$ scale is marked at the left corner and it is the same in both images. **Right:** The hard (2-7 keV) band image. It is dominated by the unresolved core.

Holt, Tadhunter & Morganti (2003). The X-ray emission is also stretched towards the South-West similarly to the optical emission and is aligned also agrees with the VLBI jet axis (Stanghellini et al. 2001) suggesting that it may be related to the expanding GPS source. More detailed discussion is presented in Guainazzi et al. (2008 in preparation).

Interestingly there is so far no detection of a hot ($kT \sim$ a few keV) cocoon that is predicted by theoretical models of the expanding radio source. Is this because we did not observe the right targets or we are limited by the spatial resolution of the telescopes. O'Dea et al. (2006) reported a thermal component in an XMM-Newton spectrum of 3C303.1 ($z=0.267$). They suggest that this thermal emission could be due to plasma heated by the shock of the expanding radio source. The source is unresolved in this X-ray observation and only the spectrum could be used to disentangle the emission components. Future *Chandra* observation may allow for more detailed investigations of the X-ray properties on a few arcsec scales.

4 Conclusions and Future Perspectives

A number of pointed X-ray observations of GPS and CSS sources has increased significantly over the last decade. However, a complete sample is still not available and there is therefore no statistically solid and systematic study of the X-ray properties of such a sample. The current observed trends need to be confirmed in the future. We are continuing our efforts to obtain X-ray observations of all the GPS sources in Stanghellini et al. (1998) and making a slow progress.

There are many remaining questions as we do not know answers to the observed correlations, the processes dominating X-ray emission, radio source environment. The basic questions about the nature of the activity is still not answered: Is the radio source intermittent? Is the source short

lived? Does the GPS radio structure fade away? Many questions that have been asked at this workshop were related to the source nature and evolution. They have to be investigated using multi-wavelength data. Samples that cover radio-optical-UV-X-rays- γ -rays are needed to test models and understand source nature and connection to a population of large scale radio sources.

There are plans for future X-rays and γ -rays missions that will become active and provide new information about the high energy processes in the GPS sources. FERMI (GLAST) has been successfully launched this year. This is the first γ -ray instrument capable of detecting GPS sources if they emit γ -rays. FERMI will collect the data at γ -ray energies $> 10^{22}$ Hz) that may provide tests and possible constraints on the emission processes from the GPS radio lobes predicted by Stawarz et al (2008).

New high energy X-ray missions with a large collective area such as NuStar (Harrison et al. 2005, Koglin et al. 2005) and EXIST (Grindlay 2007) are being built and will become available in the near future. They will be capable of detecting X-ray emission from GPS/CSS sources and will provide low resolution X-ray spectra at energies > 10 keV for the first time. The high resolution X-ray spectra will become available in the next decade when the X-ray International Observatory (IXO) is placed on orbit. This new mission will also have good imaging capabilities. However, the highest resolution X-ray spectra will allow for detailed studies of the absorption and emission line structure, so will give information about properties of the gas intrinsic to the source and also of a thermal emission components. For example we will be able to distinguish between the shock heated plasma emission and the synchrotron non-thermal emission in 3C303.1 presented by O'Dea (2008) at this workshop.

Acknowledgements. SOC and LOC members are acknowledged for organization of a great meeting. This research is funded in part by NASA contract NAS8-39073 and grant NNX07AQ55G. Partial support for this work was provided by the National Aeronautics and Space Administration through Chandra Award Number GO5-6113X, GO7-8103X-R issued by the Chandra X-Ray Observatory Center, which is operated by the Smithsonian Astrophysical Observatory for and on behalf of NASA under contract NAS8-39073.

References

- Antonelli, L. A., Fiore, F.: 1997, *Memorie della Societa Astronomica Italiana*, 68, 299
- Baum, S. A., O'Dea, C. P., de Bruyn, A. G., Murphy, D. W.: 1990, *A&A*, 232, 19
- Begelman, M. C., Cioffi, D. F. 1989: *ApJ*, 345, L21
- Begelman, M. C.: 1997, "The Most Distant Galaxies" (Dordrecht: Reidel), *Proceedings of the KNAW Colloquium held in Amsterdam, October 15-17, 1997*, *ArXiv Astrophysics e-prints*, arXiv:astro-ph/9712107
- Bicknell, G. V., Sutherland, R. S.: 2006, *AN*, 327, 235
- Elvis, M., et al.: 1994, *ApJS*, 95, 1
- Guainazzi, M. et al.: 2008, in preparation
- Guainazzi, M., Siemiginowska, A., Stanghellini, C., Grandi, P., Piconcelli, E., Azubike Ugwoke, C.: 2006, *A&A*, 446, 87
- Guainazzi, M., Siemiginowska, A., Rodriguez-Pascual, P., Stanghellini, C.: 2004, *A&A*, 421, 461
- Grindlay, J. E.: 2007, *The Central Engine of Active Galactic Nuclei*, 373, 711
- Harrison, F. A., et al.: 2005, *Experimental Astronomy*, 20, 131
- Heinz, S., Reynolds, C. S., Begelman, M. C.: 1998, *ApJ*, 501, 126
- Jester, S., Harris, D. E., Marshall, H. L., Meisenheimer, K.: 2006, *ApJ*, 648, 900
- Holt, J., Tadhunter, C. N., Morganti, R.: 2003, *MNRAS*, 342, 227
- Kirsch, M. G. F., et al.: 2004, *Proc. SPIE*, 5488, 103
- Kraft, R. P., et al.: 2007, *ApJ*, 665, 1129
- Koglin, J. E., et al.: 2005, *Proc. SPIE*, 5900, 266
- O'Dea, C. P., Mu, B., Worrall, D. M., Kastner, J., Baum, S., de Vries, W. H.: 2006, *ApJ*, 653, 1115
- O'Dea, C. P., De Vries, W. H., Worrall, D. M., Baum, S. A., Koekemoer, A.: 2000, *AJ*, 119, 478
- O'Dea, C. P.: 1998, *PASP*, 110, 493
- Ostorero, L., et al. 2008, *this Proceedings*
- Pihlström, Y. M., Conway, J. E., Vermeulen, R. C.: 2003, *A&A*, 404, 871
- Reynolds, C. S., Heinz, S., Begelman, M. C.: 2001, *ApJ*, 549, L179
- Scheuer, P. A. G.: 1974, *MNRAS*, 166, 513
- Siemiginowska, A., LaMassa, S., Aldcroft, T. L., Bechtold, J., Elvis, M.: 2008, *ApJ*, 684, 811
- Siemiginowska, A., Stawarz, Ł., Cheung, C. C., Harris, D. E., Sikora, M., Aldcroft, T. L., Bechtold, J.: 2007, *ApJ*, 657, 145
- Siemiginowska, A., Cheung, C. C., LaMassa, S., Burke, D. J., Aldcroft, T. L., Bechtold, J., Elvis, M., Worrall, D. M.: 2005, *ApJ*, 632, 110
- Siemiginowska, A., et al.: 2003, *ApJ*, 595, 643
- Siemiginowska, A., Aldcroft, T. L., Bechtold, J., Brunetti, G., Elvis, M., Stanghellini, C.: 2003, *Publications of the Astronomical Society of Australia*, 20, 113
- Siemiginowska, A., Bechtold, J., Aldcroft, T. L., Elvis, M., Harris, D. E., Dobrzycki, A.: 2002, *ApJ*, 570, 543
- Sikora, M., Stawarz, Ł., Lasota, J.-P.: 2007, *ApJ*, 658, 815
- Smith, D. A., Wilson, A. S., Arnaud, K. A., Terashima, Y., Young, A. J.: 2002, *ApJ*, 565, 195
- Stanghellini, C., O'Dea, C. P., Dallacasa, D., Baum, S. A., Fanti, R., Fanti, C.: 1998, *A&AS*, 131, 303
- Stanghellini, C., Dallacasa, D., O'Dea, C. P., Baum, S. A., Fanti, R., Fanti, C.: 2001, *A&A*, 377, 377
- Stawarz, Ł., Ostorero, L., Begelman, M. C., Moderski, R., Kataoka, J., Wagner, S.: 2008, *ApJ*, 680, 911
- Stawarz, Ł.: 2004, *ApJ*, 613, 119
- Stawarz, Ł., Sikora, M., Ostrowski, M., Begelman, M. C.: 2004, *ApJ*, 608, 95
- Sutherland, R. S., Bicknell, G. V.: 2007a, *ApJS*, 173, 37
- Sutherland, R. S., Bicknell, G. V.: 2007b, *Ap&SS*, 311, 293
- Tengstrand, O., Guainazzi, M., Siemiginowska, A., Fonseca Bonilla, N., Labiano, A., Worrall, D., Grandi, P., Piconcelli: 2008, *A&A*, submitted
- van Speybroeck, L. P., Jerius, D., Edgar, R. J., Gaetz, T. J., Zhao, P., Reid, P. B.: 1997, *Proc. SPIE*, 3113, 89
- Vink, J., Snellen, I., Mack, K.-H., Schilizzi, R.: 2006, *MNRAS*, 367, 928
- Weisskopf, M. C., Tananbaum, H. D., Van Speybroeck, L. P., O'Dell, S. L.: 2000, *Proc. SPIE*, 4012, 2
- Wilson, A. S., Young, A. J., Shopbell, P. L.: 2000, *ApJ*, 544, L27

Worrall, D. M., Hardcastle, M. J., Pearson, T. J., Readhead,
A. C. S.: 2004, MNRAS , 347, 632